# Quantum mechanical calculations of fusion reactions induced by multi-neutron halo systems below and above Coulomb barrier

Fatima M. Hussain and Fouad A. Majeed*

Department of Physics,
College of Education for Pure Sciences,
University of Babylon,
Babylon, Iraq
Email: fathussainnn@gmail.com
Email: fmajeed@uobabylon.edu.iq
*Corresponding author

**Abstract:** The role of breakup channel in fusion reactions involving two and four neutron halos is discussed in this paper. The cross-sections $\sigma_{fus}$, barrier distributions $D_{fus}$, probability of fusion $P_{fus}$, and the mean angular momentum ($L$) were calculated utilising quantum mechanics by means of the CC code. The systems $^{4}$He+$^{65}$Cu, $^{6}$He+$^{64}$Zn and $^{6}$He+$^{197}$Au were used as base systems to study the fusion reaction for the systems $^{6}$He+$^{65}$Cu, $^{8}$He+$^{65}$Cu, $^{6}$He+$^{63}$Cu, $^{6}$He+$^{192}$Os to understand the effect of breakup of $^{6}$He and $^{8}$He halo nuclei. The Woods-Saxon parameters for the studied systems were fitted using the $\chi^2$ method to fit the centroid to the experimental height barrier $V_b$. The comparison of theoretical results with the corresponding experimental data shows clearly that for these halo systems the breakup channel plays crucial role in the calculations and should be taken into consideration to enhance the calculations especially below the Coulomb barrier $V_b$.

**Keywords:** fusion cross-section; mean angular momentum; fusion barrier distribution; breakup channel.

**Reference** to this paper should be made as follows: Hussain, F.M. and Majeed, F.A. (2021) 'Quantum mechanical calculations of fusion reactions induced by multi-neutron halo systems below and above Coulomb barrier', *Int. J. Nuclear Energy Science and Technology*, Vol. 15, No. 1, pp.23–35.

**Biographical notes:** Fatima M. Hussain is an Assistant Professor at University of Babylon. Her fields of expertise are fusion reaction both elastic and inelastic. She obtained her BSc degree in Physics from University of Babylon (2005) and MSc in Nuclear Physics from University of Kufa.

Fouad A. Majeed obtained his BSc degree in Physics from Al-Mustansiriyah University, College of Science (1997), MSc (2000) and PhD (2005) in Theoretical Nuclear Physics from College of Science, Al-Nahrain University. He is a Professor at University of Babylon. He has received awards as a Visiting Scientist from The Abdus Salam (ICTP) and Post-Doctoral Fellow from TWAS-CNPq. His fields of expertise are study of nuclear reactions and nuclear structure.

## 1 Introduction

The fusion reaction of weakly bound nuclei is one of the interesting topics nowadays with the advancements of radioactive beam facilities. The main question is still under investigation whether the fusion cross-section is enhanced due to large cross-section of fusion for these nuclei (Vinodkumar et al., 2013). The height of fusion barrier is significantly affect on fusion cross-sections, the barrier consists of the Coulomb and nuclear potentials. The repulsive Coulomb energy is supplied by the atomic numbers of the projectile and the target nuclei, as for the mass numbers are connected to the attractive nuclear energy. If fallen flux on barrier is less than the barrier height, more of fallen energy does not pass through the interaction barrier and elastic scattering occurs. When the quantum tunnelling occurs, the fusion process is produced between two nuclei. Also, the increase in incident flow helps improve cross-sections of fusion (So, 2011; Choi et al., 2018). Lately, various unstable isotopes neutron-abundant nuclei, like $^{6,8}$He, $^{9,11}$Li, $^{11}$Be and $^{16,19}$C, have been created which is due to the progress in the technique of isotopes with unstable nuclides. The fusion mechanism of such isotopes has given a lot of interest. In fact, many practical measurements have been made for cross-sections of total fusion, e.g., $^{6}$He+$^{209}$Bi (Choi et al., 2018; Kolata et al., 1998; Hassan et al., 2006), $^{11}$Be+$^{209}$Bi (Signorini et al., 2004), $^{11}$Li+$^{208}$Pb (Vinodkumar et al., 2013), $^{6}$He+$^{238}$U (Raabe et al., 2004), $^{6,8}$He+$^{197}$Au (Lemasson et al., 2009) and $^{15}$C+$^{232}$Th (Alcorta et al., 2011) reactions. The breakup processes of nuclei with neutron-rich halo construction were studied by achieving several theoretical calculations at lower energy (Canto et al., 2006, 2015; Diaz-Torres and Thompson, 2002; Hagino et al., 2000; Ito et al., 2006).

An appearance of radiation beams has enhanced this concern because modern specifications are interested with several of these isotopes, especially with the weakly bound that at most available so far, imply that (Signorini et al.,2004):

1) *Halo*: The last nucleon weakly bound at most in the *s*-states wavefunction which have verry long tail expanded behind the core $^{4}$He nucleus. This result in many states with different maximum values of r.m.s. radii which deviates from the elation $r_0A^{1/3}$ systematics with ($r_0$∼1.18 fm) used for most stable nuclei. This phenomenon is found in many light nuclei such as, $^{11}$Be and $^{11}$Li (Signorini et al., 2004; Tanihata et al., 1985; Tanihata, 1996).

2) *Shell*: The last nucleons spin in the shell away from the core. The case is of $^{6}$He, $^{8}$He (Tanihata et al., 1992; Alkhazov et al., 1997). Identical constructions were expected in neutron abundant nuclei by any relativistically mean field enumeration (Suzuki et al., 1995), they are performed in sodium nuclei (Signorini et al., 2004; Fukunishi et al., 1993) and expected in aluminium nuclei (Ozawa et al., 2002).

3) Last nucleons have weakly linked energy, which is a common characteristic and it is obviously expected in all the radioactive nuclei close to the limits of the stable nuclei.

The above characteristics are reliant on each other, especially the halo format is tightly connected to a weakly linking energy of the valence nucleons. Cross-sections of fusion

can be improved or suppressed when the above features output an opposing or disagreeing influence of the fusion mechanism about fusion barrier (Signorini et al., 2004). The halo-nucleus $^{6}$He presents the peculiar properties and has a relatively small breakup threshold (the two-neutron separation energy is $S_{2n}$ = 0.973MeV) (Raabe et al., 2004). The multi-neutron halo nuclei such as $^{8}$He in addition to $^{6}$He have increasing segregation energy quite different in demeanour from the other nuclei. In the empirical and theoretical difficulties related with $^{8}$He produce complicated trouble when the review of the tunnelling of this nucleus with the highest neutrons or protons ratio (Lemasson et al., 2009). Majeed and Abdul-Hussien (2016) investigated the role of the break-up channel in the semiclassical theory for $^{6;8}$He halo neutron nuclei, which have impact of their calculations of the fusion cross-sections $\sigma_{fus}$, and the fusion barrier distribution $D_{fus}$. Majeed et al. (2017) compared semi-classical and quantum theories of fusion reactions in medium and heavy nuclei $^{46}$Ti+$^{46}$Ti and $^{58}$Ni+$^{58}$Ni with $^{40}$Ar+$^{144}$Sm, $^{40}$Ar+$^{148}$Sm and $^{40}$Ar+ $^{154}$Sm, they proved that the coupled channels involved in semi-classical have an effective role in producing in the total fusion reaction cross-sections $\sigma_{fus}$ and the fusion barrier distribution $D_{fus}$ around fusion barrier in Majeed et al. (2017) and Hussain et al. (2019a). The influence of the breakup channel on systems loosely bound light systems by virtue of a quantum mechanics and semi-classical theories has been debated by Majeed (2017). And in other studies, Majeed et al. (2019) described fusion barrier distribution results for $^{40}$Ca +$^{192}$Os, $^{40}$Ca + $^{194}$Pt, and $^{48}$Ca + $^{197}$Au reactions by applying a Wong formula using full quantum mechanical model. Hussain et al. (2019b) studied coupled channel mechanism of two quantum mechanical approaches for light stable nuclei.

In this study, the effect of the breakup channel will be investigated for the systems $^{4}$He+$^{65}$Cu, $^{6}$He+$^{65}$Cu, $^{8}$He+$^{65}$Cu, $^{6}$He+$^{63}$Cu , $^{6}$He+$^{64}$Zn, $^{6}$He+$^{192}$Os and $^{6}$He+$^{197}$Au that included multi-nucleon halo nuclei. The study will be conducted using the quantum mechanical model using the CC code and the results will be compared with the measured data.

## 2 Theoretical framework

The valence neutron action is achieved by determining the distance with radius, and barrier height of interaction potential. This parameters $R_B$ ($r_B$) and $V_B$ were found by employing the total potential of optical model as in equation (So et al., 2013).

$$V_T^{\ell}(r) = V_C(r) + V_N(r) + V_{\ell}(r) \tag{1}$$

Here, $V_C$ and $V_N$ are the Coulomb and the nuclear with $V_{\ell}$ central potentials, respectively. The nuclear potential is combined of two fractions, as given

$$V_N(r) = V(r) + iW(r) = V_0 f_V(r) + iW_0 f_w(r)$$

$V_0$ and $W_0$ are the depths of the real and imaginary parts of the potentials with the Woods–Saxon form $f_V(r) = [1 + e^{(r-R_i)/a_i}]^{-1}$ with $i = V$ and $W$ .

Depending on Wong formula (Wong, 1973), the cross-sections form expressions of angular-momentum partial waves, for distorted and directed nuclei (with direction angles $\theta_i$), being in same planes, with collision energy $E_{c.m.}$ is

$$\sigma\left(E_{c.m.}.\theta_i\right)=\sum_{\ell=0}^{\ell_{max}}\sigma_\ell=\frac{\pi}{k^2}\sum_{\ell=0}^{\ell_{max}}\left(2\ell+1\right)P_\ell\left(E_{c.m.}.\theta_i\right) \tag{3}$$

with $k=\sqrt{\frac{2\mu E_{c.m.}}{\hbar^2}}$ and $\mu$ is the reduced mass, $P_\ell$ is the transmission coefficient for each $\ell$ which describe the penetrability of barrier, assuming that projectile is a particle separated from the core. When it interacts with the target nucleus, its status will be disordered, also the strengths of the target appear quite differently on the particle and the core. If one separates the projectile-target interaction into $V_C\left(r_C\right)$, the interaction of the target nucleus with the core, and $V_N\left(r'\right)$, the interaction of the target nucleus with the particle, then there is a mechanism for coupling ground and inelastic (continuum) states together (Nunes and Thompson, 1999).

To characterise the breakup process of nuclei like $^{6,8}$He, the function excitations in the 2n, 4n+$^4$He reactions start than the ground level $\phi_{gs}\left(r\right)$ to excited levels in the status $\upsilon_{\ell sj.k}\left(r\right)$, for some momentum $k$ and partial waves $\ell$. The use of singular energy eigenfunctions, therewith, the results of the inelastic form factors which will not converge, as the continuum wave functions do not degrade to zero as $r\to\infty$ suitably speedy to be square integrable. The solution (Nunes and Thompson, 1999; Sakuragi et al., 1986) to transaction with this variation is to choose excitation states, not at a singular energy, but mean over cramped range of energies, where these ‘‘bins’’ cases are square integrable. We distinguish these bin cases by their wavenumber boundaries $\left[k_1.\,k_2\right]$ and their angular momentum quantum numbers $\left(\ell s\right)j$. They have been utilised in the Coupled Discretised Continuum Channels (CDCC) theory.

The radial wave functions fulfil the set of coupling equations

$$\begin{aligned}&\left[-\frac{\hbar^2}{2\mu}\left(\frac{d^2}{dr^2}-\frac{\ell\left(\ell+1\right)}{r^2}\right)+\mathcal{E}\left(\left[k_1.\,k_2\right]\right)-E\right]\mathcal{F}_{\alpha J}\left(r\right)\\&+\sum_{\alpha}^{\cdot}i^{\ell-\ell}V_{\alpha:\alpha'}^{J}\left(r\right)\mathcal{F}_{\alpha' J}\left(r\right)=0\end{aligned} \tag{4}$$

where $\mathcal{E}\left(\left[k_1.\,k_2\right]\right)$ indicates the mean energy of continuum bins $\left[k_1.\,k_2\right]$ or $\mathcal{E}<0$ for the ground status, and $V_{\alpha.\alpha}^{J}\left(r\right)$ depicts the coupling between the various proportional movement statuses.

$$V_{\alpha:\alpha'}^{J}=\varphi_\alpha\left(r\right)|V_C\left(r_C\right)+V_N\left(r'\right)+V_\ell\left(r\right)|\varphi_{\alpha'}\left(r\right) \tag{5}$$

In equation (4) the equations of coupled status may be disbanded precisely if they are not so numerous. Moreover, repetitive extensions are utilised starting with $\mathcal{F}^{-1}(r)=0$, and ongoing as

$$\left[-\frac{\hbar^2}{2\mu}\left(\frac{d^2}{dr^2}-\frac{\ell(\ell+1)}{r^2}\right)+V^J_{\alpha:\alpha}(r)+\mathcal{E}\left(\left[k_1.\,k_2\right]\right)-E\right]\mathcal{F}^{(n)}_{\alpha J}(r) = \sum_{\alpha\neq\alpha} i^{\ell-\ell}V^J_{\alpha:\alpha'}(r)\mathcal{F}^{(n-1)}_{\alpha J}(r) \tag{6}$$

where $\mathcal{F}^{(0)}(r)$ indicate to the function of elastic channel, also the asymptotic notation of matrix $S^{(n)}$ of the functions $\mathcal{F}^{(n)}(r)$ at $n=0;1...$ .makes the cross-sections for *n*-th-order DWBA. The wave function of bin is given by:

$$\varphi_{\ell sj.[k_1.k_2]}(r)=\sqrt{\frac{2}{\pi N}}\int_{k_1}^{k_2} w(k)e^{-i\delta_k}\upsilon_{\ell sj.k}(r)\,dk \tag{7}$$

where $\delta_k$ is the scattering phase shift for $\upsilon_{\ell sj.k}(r)$. The normalisation constant is $N=\int_{k_1}^{k_2}\left|w(k)\right|^2 dk$ for the presumed weight function $w(k)$, were chosen to be either unity for non-*s*-wave bins or *k* for *s*-wave bins. Their cases are normalised $\varphi|\varphi=1$ time an appropriately big radius $r_{bin}$ for *r* is chosen. They are orthogonal to any tight statuses, and are orthogonal to other bin statuses if its energy scales do not interfere. The phase factor $e^{-i\delta_k}$ guarantees that they are actual valued for actual potentials $V(r)$.

Equation (6) is disbanded with an accustomed scattering border conditions (Diaz-Torres and Thompson, 2002). The fusion cross-sections $\sigma_{tot}$ is described in terms of hat quantity of influx which quits the coupling channels set due to the short-range imaginary potential $iW(r)$. When the target's stripped nucleus merges completely with the projectile's nucleus, leads to full-fusion process (Hagino et al., 2000), the cross-section for the full-fusion may be considered as the absorption cross-section by the restricted channels in the projectile (full-fusion from both ground state and excitation state) as explained in equation (3), therefore the full-fusion probability $P_\ell$ is given as (Diaz-Torres and Thompson, 2002; Balantekin and Takigawa, 1998)

$$P_\ell=\frac{8}{\hbar(2E/\mu)^{1/2}}\sum_{\alpha(\mathcal{E}_\alpha<0)}\int_0^\infty\left|\mathcal{F}^{(n)}_{\alpha J}(r)\right|^2\left[-W(r)\right]dr \tag{8}$$

and the average angular momentum

$$\ell(E_{c.m.})=\frac{\sum_{\ell=0}^{\ell_{max}}\ell\sigma_\ell(E_{c.m.})}{\sum_{\ell=0}^{\ell_{max}}\sigma_\ell(E_{c.m.})} \tag{9}$$

A substitute method of evaluating the measured cross-section values is to look at the second energy derivative of the magnitude $E\sigma$ is known the barrier distribution. To

explain on the physical importance of this magnitude we treat penetration probabilities for various partial waves in the status of coupling to an internal system. Under certain conditions, to be explained in the following section, this can approach the $\ell$ requirement of the transmission probability at a taken energy by easily diversion the energy

$$P_\ell \cong P_0\left[E-\frac{\ell(\ell+1)\hbar^2}{2\mu R^2(E)}\right] \tag{10}$$

As $\mu R^2(E)$ describes an active moment of inertia. $R(E)$ was located to be a tardily changing function of energy. Then, in several purposes $R(E)$ is exchanged by $r_0$, the location of the barrier height, in equation (10). If several values of $\ell$ are significant in the set all partial-wave penetration probabilities in equation (3), we can approach that set with an integral all $\ell$, utilising equation (10) find (Balantekin and Takigawa 1998)

$$E\sigma = \pi R^2(E)\int_{-\infty}^{E} dE' P_0(E') \tag{11}$$

penetration probability is approach prorated to the second derivative of the amount $E\sigma$ up to improvements arising than the energy reliance of $R(E)$

$$\frac{dP_0(E)}{dE} \sim \frac{1}{\pi R^2(E)}\frac{d}{dE^2}\left(E\sigma(E)+\Theta\left(\frac{dR}{dE}\right)\right) \tag{12}$$

The term $\frac{dP_0(E)}{dE}$ can be more expanded and can be chosen to account for the distribution of the fusion barrier, because of the coupling to the additional degrees of freedom that will be included.

## 3 Results and discussion

In order to study the Coulomb excitations on multi-neutron halo nuclei in the fusion processes for systems have few measured data. Several systems rich with experimental data had been used to find the Woods-Saxon parameters which have close mass numbers. All calculations were performed within the full quantum mechanical model and parameters of real and imaginary nuclear potential of Woods-Saxon potential as given in Table 1.

**Table 1** Parameters of real and imaginary nuclear potential and height of barrier

| *Reactions* | $V_0$ *MeV* | $r_0$ *fm* | $a_0$ *fm* | $W_0$ *MeV* | $r_i$ *fm* | $a_i$ *fm* | $V_b$ *MeV* |
|---|---|---|---|---|---|---|---|
| $^{4}$He+$^{65}$Cu | 29.5 | 0.945 | 0.445 | 9.80 | 0.919 | 0.789 | 20.40 |
| $^{6}$He+$^{65}$Cu | | | | | | | |
| $^{8}$He+$^{65}$Cu | | | | | | | |
| $^{6}$He+$^{63}$Cu<br>$^{6}$He+$^{64}$Zn | 57.1 | 1.073 | 0.736 | 19.0 | 0.927 | 0.784 | 8.60 |
| $^{6}$He+$^{192}$Os<br>$^{6}$He+$^{197}$Au | 236.6 | 1.00 | 0.50 | 78.9 | 0.929 | 0.783 | 21.34 |

### *3.1 The $^{6}He+^{65}Cu$ and $^{8}He+^{65}Cu$ systems*

The $^{4}He+^{65}Cu$ system is taken to be as base system to estimate the Woods-Saxon parameters for the systems $^{6}He+^{65}Cu$ and $^{8}He+^{65}Cu$, which consist of two and four halo neutrons as a projectile fuse with the target $^{65}Cu$. The estimated parameters chosen of these systems are tabulated in Table 1. The measured data of $^{4}He+^{65}Cu$ system for the cross-section as function of centre of mass energy is taken from (Navin et al., 2004). Figures 1 and 2 displays the comparison of the calculated cross-sections $\sigma_{fus}$, barrier distributions $D_{fus}$, probabilities $P_{fus}$ and mean angular momentum <L> for the two cases where the breakup channel included and not included in the calculations. Panel (a) of Figure 1, illustrates the curves of the theoretical cross-sections in no coupled and coupled states compared with empirical values, we found excellent match above and under barrier by chi square values are (0.01139806, 0.05264974) for $^{8}He+^{65}Cu$ but less match in the values of $^{6}He+^{65}Cu$ are (0.04500791, 0.16428200) and values of $^{6}He+^{65}Cu$ are (0.17030210, 0.42961800), where the breakup of 4n halo nucleus coupled with reaction channels to produced perfect match. Panel (b) appears the best match of original system $^{4}He+^{65}Cu$ in barrier distribution values, as for the location of peaks to Coulomb barrier energy are very close of these systems. We find that system $^{4}He+^{65}Cu$ is very appropriate choice as base system to find the best fitted Woods-Saxon parameters used for $^{6}He+^{65}Cu$ and $^{8}He+^{65}Cu$ calculations.

**Figure 1** The empirical values (black circles) from Navin et al. (2004) for $^{4}He+^{65}Cu$ system compared with the quantum mechanical results using CC code. The dash and solid curves are for the no coupling and coupling results, (blue colour) $^{4}He+^{65}Cu$, (red colour) $^{6}He+^{65}Cu$ and (orange colour) $^{84}He+^{65}Cu$, respectively, compared with data. (a) for the total fusion cross-section $\sigma_{fus}$ (mb) and (b) for the fusion barrier distribution $D_{fus}$ (mb/MeV)

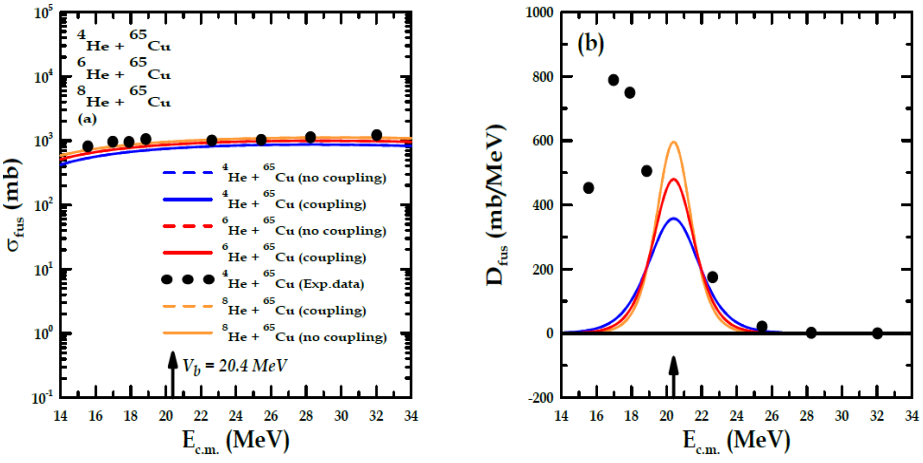


Figure 2, panels (c) and (d) review the theoretical curves of tunnelling probabilities $P_{fus}$ and the mean angular momentum <L> for $^{4}He+^{65}Cu$, $^{6}He+^{65}Cu$ and $^{8}He+^{65}Cu$ compared to the measured values. The tunnelling probabilities and measured data perfectly matched for the system $^{4}He+^{65}Cu$ in the case the effect of the breakup is included above the

Coulomb barrier $V_B$. All the studied systems $^4$He+$^{65}$Cu, $^6$He+$^{65}$Cu and $^8$He+$^{65}$Cu the calculations the mean angular momentum <L> is not agreed with the experimental data below the Coulomb barrier $V_B$ indicated by the black arrow in the $E_{c.m.}$ axis.

**Figure 2** The empirical values (black circles) are compared with the quantum mechanical results using CC code. The dash and solid curves are for the no coupling and coupling results, (blue colour) $^4$He+$^{65}$Cu, (red colour) $^6$He+$^{65}$Cu and (orange colour) $^8$He+$^{65}$Cu, respectively, compared with data. (c) for the tunnelling probabilities $P_{fus}$ and (d) for the mean angular momentum <L>.

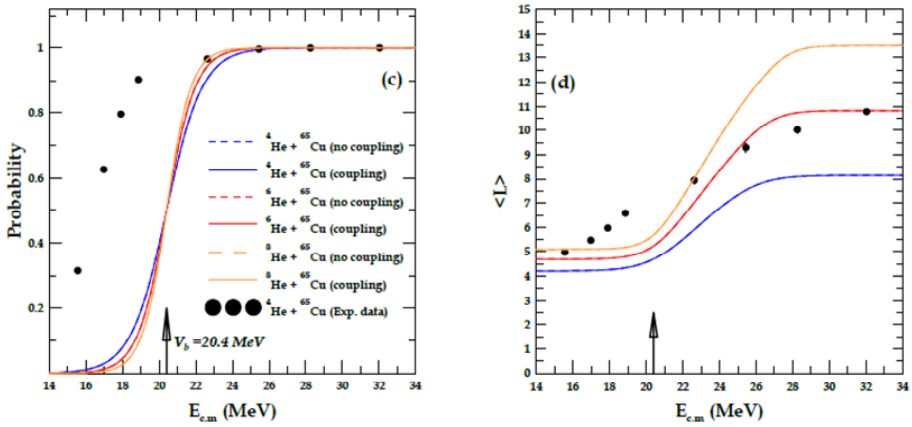


## 3.2 *The $^6$He+$^{63}$Cu system*

The base system is $^6$He+$^{64}$Zn has been chosen to fit the Woods-Saxon parameters tabulated in Table 1, that is used for the calculations of $^6$He+$^{63}$Cu system. The projectile is the same while the targets are different. The results of cross-sections $\sigma_{fus}$, barrier distributions $D_{fus}$, tunnelling probabilities $P_{fus}$ and mean angular momentum <L> are displayed in Figure 3, panels (a) and (b) and Figure 4, panels (c) and (d), respectively. There is one experimental value below the barrier height $V_b$ for $\sigma_f$, therefore we cannot make clear judgment if the calculation successful below the Coulomb barrier $V_b$, while the calculations overestimated the measured data above $V_b$. The coupling that involved breakup channel is supported the calculations very well down barrier energy, with similar parameters and barrier height are chosen in original and virtual systems. From the comparison between two system with empirical data from Fisichella et al. (2011), the best matching value of chi-square values in no and coupling state under barrier is (0.01146328) of original system and (0.12500000, 0.04548522) in two states of virtual system, while above barrier all cross-section calculations are shifted to top data due to increased angular momentum values. The effect of the breakup was evident in part b, which gave multiple peaks of barrier with more match above barrier in $^6$He+$^{65}$Zn system, and single peak shows in$^6$He+$^{63}$Cu system, it is also closer to data around barrier.

**Figure 3** The empirical values (black circles) from Fisichella et al. (2011) for $^{6}$He+$^{65}$Zn system compared with the quantum mechanical results using CC code. The dash and solid curves are for the no coupling and coupling results, (blue colour) $^{6}$He+$^{63}$Cu and (red colour) $^{6}$He+$^{65}$Zn, respectively, both compared with data. (a) for the total fusion cross-section $\sigma_{fus}$ (mb) and (b) for the fusion barrier distribution $D_{fus}$ (mb/MeV)

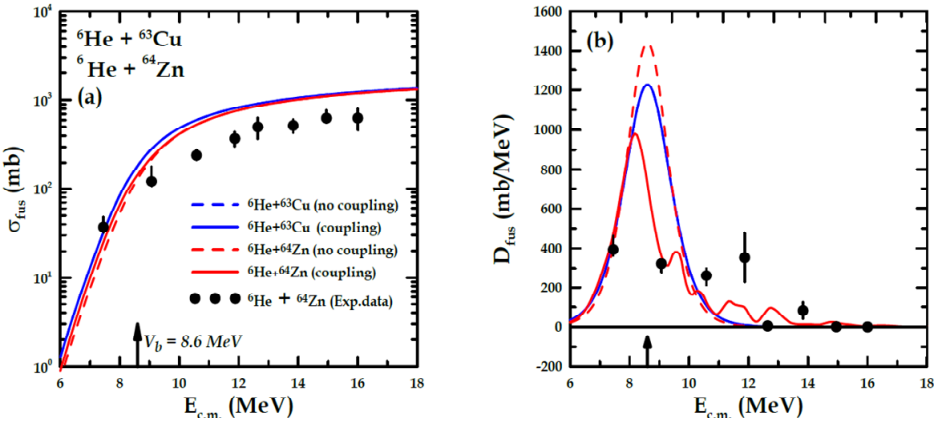


The tunnelling probabilities $P_{fus}$ and the mean angular momentum <L> are shown in Figure 4, panels (c) and (d), the calculation of probabilities under barrier indicated to clear agreement between the two systems with experimental data. Although the calculations have rambles, it is still very close to the experimental data. However, including the coupling the calculations of the mean angular momentum <L> for the system $^{6}$He+$^{64}$Zn is overshooting the experimental data.

**Figure 4** The empirical values (black circles) are compared with the quantum mechanical results using CC code. The dash and solid curves are for the no coupling and coupling results, (blue colour) $^{6}$He+$^{63}$Cu and (red colour) $^{6}$He+$^{64}$Zn, respectively, both compared with data. (c) for the tunnelling probabilities $P_{fus}$ and (d) for the mean angular momentum <L>

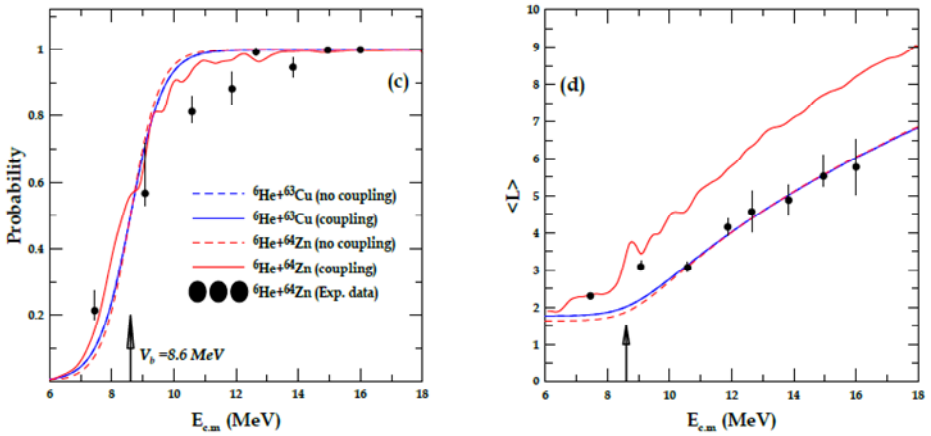

### 3.3 $^{6}He + {}^{192}Os$ system

The measured data are taken from Penionzhkevich et al. (2007) and consist of the $^{6}$He + $^{197}$Au system, that we took as base system to find the best fit of Woods-Saxon parameters. These parameters are tabulated in Table 1 which has been used to perform the calculations. The $^{6}$He nucleus which has halo structure and the breakup of two neutrons is considered in coupling channels, the parameters depend on two systems and barrier height based on empirical data. The cross-sections $\sigma_{fus}$, barrier distributions $D_{fus}$, tunnelling probabilities $P_{fus}$ and mean angular momentum <L> calculations are presented into Figure 5, panels (a) and (b) and Figure 6, panels (c) and (d), where the coupling channel shows noticeable agreement of both systems calculations with corresponding data. As in the panels (a) and (b), of cross-sections, barrier distributions, around Coulomb barrier.

In Figure 6, panel (c), the results of coupled case of fusion probabilities in excellent matching above and below the barrier energy, while no coupled case appears especially matching above barrier. In panel (d), the mean angular momentum of virtual system seems more matched and very close to the original system calculations of corresponding empirical values which in turn show the same behaviour. We have succeeded in reproducing the empirical values for virtual system based on numerical abundance of empirical values in original system.

**Figure 5** The empirical values (black circles) from Penionzhkevich et al. (2007) for $^{6}$He+$^{197}$Au system compared with the quantum mechanical results using CC code. The dash and solid curves are for the no coupling and coupling results, (blue colour) $^{6}$He+$^{192}$Os and (red colour) $^{6}$He+$^{197}$Au respectively, both compared with data. (a) for the total fusion cross-section $\sigma_{fus}$ (mb) and (b) for the fusion barrier distribution $D_{fus}$ (mb/MeV)

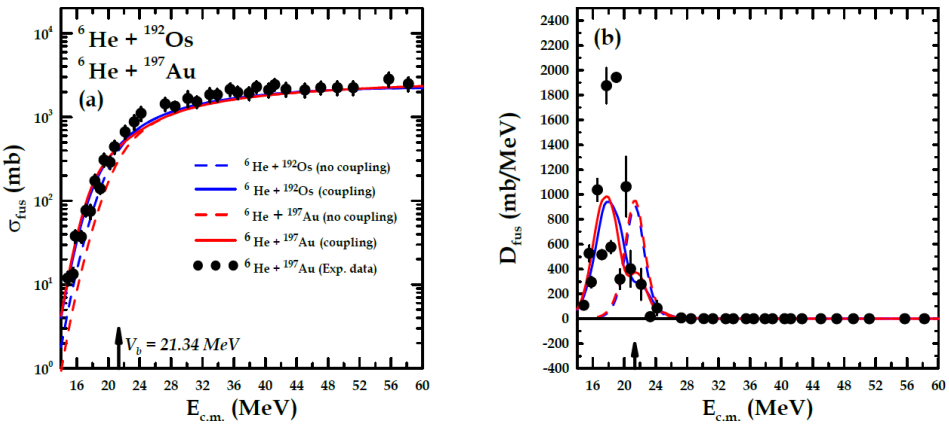

**Figure 6** The empirical values (black circles) are compared with the quantum mechanical results using CC code. The dash and solid curves are for the no coupling and coupling results, (blue colour) $^{6}$He+$^{192}$Os and (red colour) $^{6}$He+$^{197}$Au, respectively, both compared with data. (c) for the tunnelling probabilities $P_{fus}$ and (d) for the mean angular momentum <L>

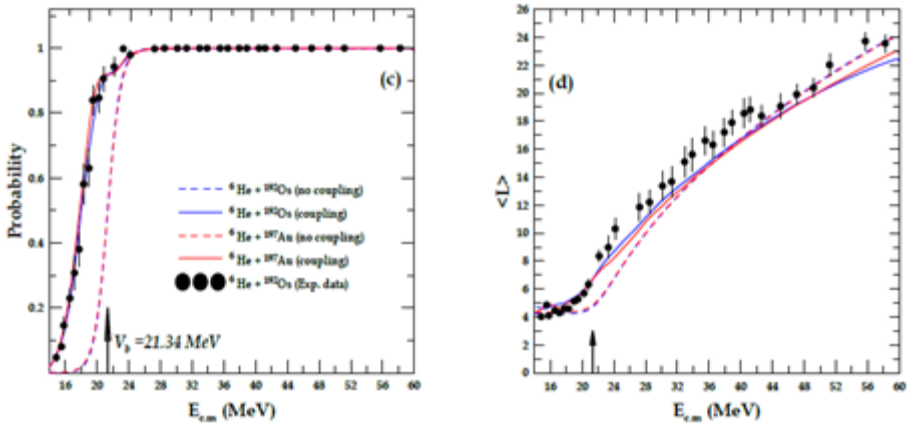


## 4 Conclusion

We have employed the quantum mechanics calculations, the fusion cross-section, barrier distributions, probabilities and mean angular momentum for systems having halo structure nuclei. The two and four halo nucleons are taken into account for virtual systems $^{6}$He+$^{63}$Cu, $^{6}$He+$^{65}$Cu, $^{6}$He+$^{192}$Os,$^{8}$He+$^{65}$Cu, respectively, which are made up of one or two empirical values. We took care to accredit original systems in energy ranges of virtual systems and close to their mass numbers. The results have been calculated by quantum mechanics CC Code including the clear effect of breakup channel which helped to improve the halo weakly bound nuclei calculations. We found from the comparison between original and virtual systems very good matching with empirical data which clearly indicates the dependence of the virtual systems as an alternative of original system.

## References

Alcorta, M., Rehm, K.E., Back, B.B., Bedoor, S., Bertone, P.F., Deibel, C.M., DiGiovine, B., Esbensen, H., Greene, J.P., Hoffman, C.R., Jiang, C.L., Lighthall, J. C., Marley, S.T., Pardo, R.C., Paul, M., Rogers, A.M., Ugalde, C. and Wuosmaa, A.H. (2011) 'Fusion reactions with the one-neutron halo nucleus $^{15}$C', *Physical Review Letters*, Vol. 106. Doi: 10.1051/epjconf/20111713003.

Alkhazov, G.D., Andronenko, M.N., Dobrovolsky, A.V., Egelhof, P., Gavrilov, G.E., Geissel, H., Irnich, H., Khanzadeev, A.V., Korolev, G.A., Lobodenko, A.A., Münzenberg, G., Mutterer, M., Neumaier, S.R., Nickel, F., Schwab, W., Seliverstov, D.M., Suzuki, T., Theobald, J.P., Timofeev, N.A., Vorobyov, A.A. and Yatsoura, V.I. (1997) 'Nuclear matter distributions in $^{6}$He and $^{8}$He from small angle *p*-He scattering in inverse kinematics at intermediate energy', *Physical Review Letters*, Vol. 78. Doi: 10.1103/PhysRevLett.78.2313.

Balantekin, A.B. and Takigawa, N. (1998) 'Quantum tunneling in nuclear fusion', *Reviews of Modern Physics*, Vol. 70. Doi: 10.1103/RevModPhys.70.77.

Canto, L., Gomes, P., Donangelo, R. and Hussein, M. (2006) 'Fusion and breakup of weakly bound nuclei', *Physics Reports*, Vol. 424, pp.1–111.

Canto, L., Gomes, P., Donangelo, R., Lubian, J. and Hussein, M. (2015) 'Recent developments in fusion and direct reactions with weakly bound nuclei', *Physics Reports*, Vol. 596, pp.1–86.

Choi, K.S., Cheoun, M.K., So, W.Y., Hagino, K. and Kim, K.S. (2018) 'Coupled-channels analyses for $^{9,11}$Li + $^{208}$Pb fusion reactions with multi-neutron transfer couplings', *Physical Letters B*, Vol. 780, pp.455–460.

Diaz-Torres, A. and Thompson, I.J. (2002) 'Effect of continuum couplings in fusion of halo $^{11}$Be on $^{208}$Pb around the coulomb barrier', *Physical Review C*, Vol. 65, pp.1–15.

Fisichella, M., Scuderi, V., Di Pietro, A., Figuera, P., Lattuada, M., Marchetta, C., Milin, M., Musumarra, A., Pellegriti, M.G., Skukan, N., Strano, E., Torresi, D. and Zadro, M. (2011) 'Halo effects on fusion cross section in $^{4,6}$He+$^{64}$Zn collision around and below the coulomb barrier', *Journal of Physics: Conference Series*, Vol. 282, pp.1–9.

Fukunishi, M., Otsuka, T. and Tanihata, I. (1993) 'Neutron-skin and proton-skin formations in exotic nuclei far from stability', *Physical Review C*, Vol. 48, pp.1648–1655.

Hagino, K., Vitturi, A., Dasso, C.H. and Lenzi, S.M. (2000) 'Role of breakup processes in fusion enhancement of drip-line nuclei at energies below the Coulomb barrier', *Physical Review C*, Vol. 61, pp1–8.

Hassan, A.A., Lukyanov, S., Kalpakchieva, R., Penionzhkevich, Y.E., Astabatyan, R., Vinsour, J., Dlouhy, Z., Kulko, A.A., Mrazek, J., Lobastov, S.P., Markaryan, E. R., Maslov, V.A., Skobelev, N.K. and Sobolev, Y.G. (2006) 'Investigation of nuclear fusion in reactions of $^{4,6}$ He and $^{7}$ Li on $^{208}$ Pb and $^{208}$ Bi nuclei', *Bulletin of the Russian Academy of Sciences: Physics*, Vol. 70, pp.1558–1563.

Hussain, F.M., Majeed, F.A. and Abdul-Hussien, Y.A. (2019a) 'Description of coupled-channel in Semiclassical treatment of heavy ion fusion reactions', *IOP Conference Series: Materials Science and Engineering*, Vol. 571. Doi: 10.1088/1757-899X/571/1/012113.

Hussain, F.M., Majeed, F.A. and Abdul-Hussien, Y.A. (2019b) 'Coupling channels mechanism of complete fusion reactions in some light stable nuclei', *AIP Conference Proce*edings, Vol. 2144. Doi: 10.1063/1.5123073.

Ito, M., Yabana, K., Nakatsukasa, T. and Ueda, M. (2006) 'Suppressed fusion cross section for neutron halo nuclei', *Physical Letters B*, Vol. 637, pp.53–57.

Kolata, J.J., Guimarães, V., Peterson, D., Santi, P., White-Stevens R., DeYoung, P.A., Peaslee G.F., Hughey B., Atalla, B., Kern, M., Jolivette, P.L., Zimmerman, J.A., Lee, M.Y., Becchetti, F.D., Aguilera, E.F., Martinez-Quiroz, E. and Hinnefeld, J.D. (1998) 'Sub-barrier fusion of $^{6}$He with $^{209}$Bi', *Physical Review Letters*, Vol. 81. Doi: 10.1103/PHYSREVLETT.81.4580.

Lemasson, A., Shrivastava, A., Navin, M., Rejmund, N., Keeley, V., Zelevinsky, S., Bhattacharyya, A., Chatterjee, G., de France, B., Jacquot, V., Nanal, Pillay, R.G., Raabe, R. and Schmitt, C. (2009) 'Modern rutherford experiment: tunneling of the most neutron-rich nucleus', *Physical Review Letters*, Vol. 103. Doi: 10.1103/PhysRevLett.103.232701.

Majeed F.A., Hussain F.M. and Abdul-Hussien Y.A. (2019) 'Enhanced calculations of fusion barrier distribution for heavy-ion fusion reactions using Wong formula', *International Journal of Nuclear Energy Science and Technology*, Vol. 13, No. 3, pp.226–241.

Majeed, F.A. (2017) 'The role of the breakup channel on the fusion reaction of light and weakly bound nuclei', *Journal of Nuclear Energy Science and Power Generation Technology*, Vol. 11, pp.218–228.

Majeed, F.A. and Abdul-Hussien, Y.A. (2016) 'Semiclassical treatment of fusion and breakup processes of $^{6,8}$He halo nuclei', *Journal of Theoretical and Applied Physics*, Vol. 10, pp.107–112.

Majeed, F.A., Hamodi, R.S. and Hussain, F.M. (2017) 'Effect of coupled channels on semiclassical and quantum mechanical calculations for heavy ion fusion reactions', *Journal of Computational and Theoretical Nanoscience*, Vol. 14, pp.2242–2247.

Navin, A., Tripathi, V., Blumenfeld, Y., Nanal, V., Simenel, C., Casandjian, J.M., de France, G., Raabe, R., Bazin, D., Chatterjee, A., Dasgupta, M., Kailas, S., Lemmon, R.C., Mahata, K., Pillay, R.G., Pollacco, E.C., Ramachandran, K., Rejmund, M., Shrivastava, A., Sida, J.L. and Tryggestad, E. (2004) 'Direct and compound reactions induced by unstable helium beams near the coulomb barrier', *Physical Review C*, Vol. 70. Doi: 10.1103/PhysRevC.70.044601.

Nunes, F.M. and Thompson, I.J. (1999) 'Multistep effects in sub-coulomb breakup', *Physical Review C*, Vol. 59. Doi: 10.1103/PhysRevC.59.2652.

Ozawa, A., Baumann, T., Chulkov, L., Cortina, D., Datta, U., Fernandez, J., Geissel, H., Hammache, F., Itahashi, K., Ivanov, M., Janik, R., Kato, T., Kimura, K., Kobayashi, T., Markenroth, K., Meister, M., Münzenberg, G., Ohtsubo, T. and Yamaguch, Y. (2002) 'Measurements of the interaction cross sections for Ar and Cl isotopes', *Nuclear Physics A*, Vol. 709, pp.60–72.

Penionzhkevich, Y.E., Astabatyan, R.A., Demekhina, N.A., Gulbekian, G.G., Kalpakchieva, R., Kulko, A.A., Lukyanov, S.M., Markaryan, E.R., Maslov, V.A., Muzychka Y.A., Oganessian, Y.T., Revenko, R.V., Skobelev, N.K., Sobolev, Y.G., Testov, D.A. and Zholdybaev, T. (2007) 'Excitation functions of fusion reactions and neutron transfer in the interaction of $^{6}$He with $^{197}$Au and $^{206}$Pb', *The European Physical Journal A*, Vol. 31, pp.185–194.

Raabe, R., Sida, J.L., Charvet, J.L., Alamanos, N., Angulo, C., Casandjian, J.M., Courtin, S., Drouart, A., Durand, D.J.C., Figuera, P., Gillibert, A., Heinrich, S., Jouanne, C., Lapoux, V., Lepine-Szily, A., Musumarra, A., Nalpas, L., Pierroutsakou, D., Romoli, M., Rusek, K. and Trotta, M. (2004) 'No enhancement of fusion probability by the neutron halo of $^{6}$He', *Letters Nature*, Vol. 431, pp.823–826.

Sakuragi, Y., Yahiro, M. and Kamimura, M., (1986) 'Microscopic coupled-channels study of scattering and breakup of light heavy-ions', *Progress of Theoretical Physics Supplement*, Vol. 89, pp.136–211.

Signorini, C., Yoshida, A., Watanabe, Y., Pierroutsakou, D., Stroe, L., Fukuda, T., Mazzocco, M., Fukuda N., Mizoi, Y., Ishihara, M., Sakurai H., Diaz-Torres, A. and Hagino, K. (2004) 'Subbarrier fusion in the systems $^{11,10}$Be+ $^{209}$Bi', *Nuclear Physics A.*, Vol. 735, pp.329–344.

So, W. (2011) 'Effect of valence neutron(s) in neutron-rich nuclei', *The Journal of the Korean Physical Society*, Vol. 59.

So, W., Kim, T., Han, M., Cho, H., Mo, B., Kim, S. and Kim, K. (2013) 'Relation between interaction distance and coulomb barrier height', *Journal of the Physical Society of Japan*, Vol. 82, Doi: 10.7566/JPSJ.82.044201.

Suzuki, T., Geissel, H., Bochkarev, O., Chulkov, L., Golovkov, M., Hirata, D., Irnich, H., Janas, Z., Keller, H., Kobayashi, T., Kraus, G., Münzenberg, G., Neumaier, S., Nickel, F., Ozawa, A., Piechaczeck, A., Roeckl, E., Schwab, W., Sümmerer, K., Yoshida, K. and Tanihata, I. (1995) 'Neutron skin of Na isotopes studied via their interaction cross sections', *Physical Review Letters*, Vol. 75, pp.3241–3244.

Tanihata, I. (1996) 'Neutron halo nuclei', *Journal of Physics G*, Vol. 22, pp.157–198.

Tanihata, I., Hamagaki, H., Hashimoto, O., Shida, Y., Yoshikawa, N., Sugimoto, K., Yamakawa, O., Kobayashi, T. and Takahashi, N. (1985) 'Measurements of interaction cross sections and nuclear radii in the light p-shell region', *Physical Review Letters*, Vol. 55, pp.2676–2679.

Tanihata, I., Hirata D., Kobayashi T., Shimoura, S. and Toki, H. (1992) 'Revelation of thick neutron skins in nuclei', *Physical Review B*, Vol. 289, pp.261–266.

Vinodkumar, M., Loveland, W., Yanez, R., Leonard M., Yao, L., Bricault, P., Dombsky, M., Kunz, P., Lassen, J., Morton, A.C., Ottewell, D., Preddy, D. and Trinczek, M. (2013) 'Interaction of $^{11}$Li with $^{208}$Pb', *Physical Review C*, Vol. 87, No. 6. Doi: 10.1103/PhysRevC.87.044603.

Wong, C.Y. (1973) 'Interaction barrier in charged-particle nuclear reactions', *Physical Review Letters*, Vol. 31, pp.776–769.